Electronic Supporting Information (ESI)

NMR Analysis of an Fe(I)-Carbene Complex with Strong Magnetic Anisotropy

Marko Damjanović[1], *Prinson P. Samuel*[2], *Herbert W. Roesky*[2], *Markus Enders*[1]*

[1] Institute of Inorganic Chemistry, Heidelberg University, Im Neuenheimer Feld 270, D-69120 Heidelberg, Germany.

[2] Institut für Anorganische Chemie, Georg-August-Universität, Tammannstrasse 4, D-37077, Göttingen, Germany.

Corresponding Author

Phone; +49-6221-54-6247. Fax: +49-6221-54161-6247.
E-mail: markus.enders@uni-heidelberg.de (M.E.)

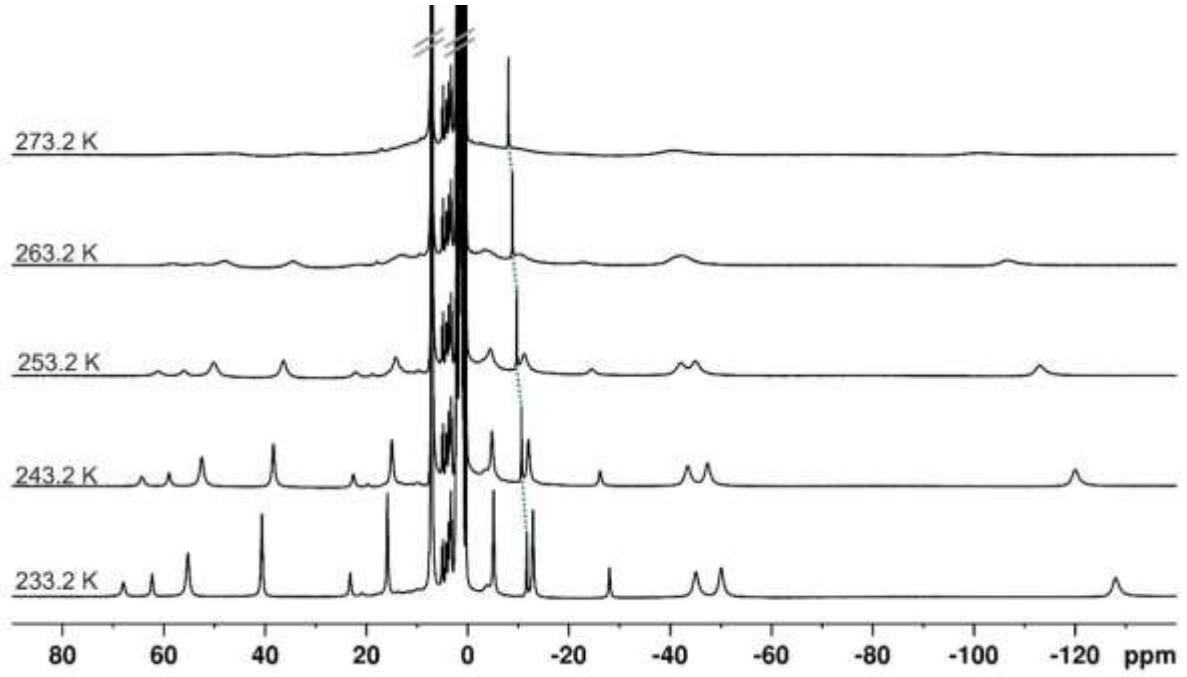

Figure S1. Variable-temperature ^{1}H NMR spectra of complex **1** (toluene-*d8*, 233.2 K to 273.2 K). At elevated temperatures, due to dynamic processes, only one paramagnetic signal remains sharp (*para*-^{1}H of Dipp- moiety (pH), marked with dotted green line).

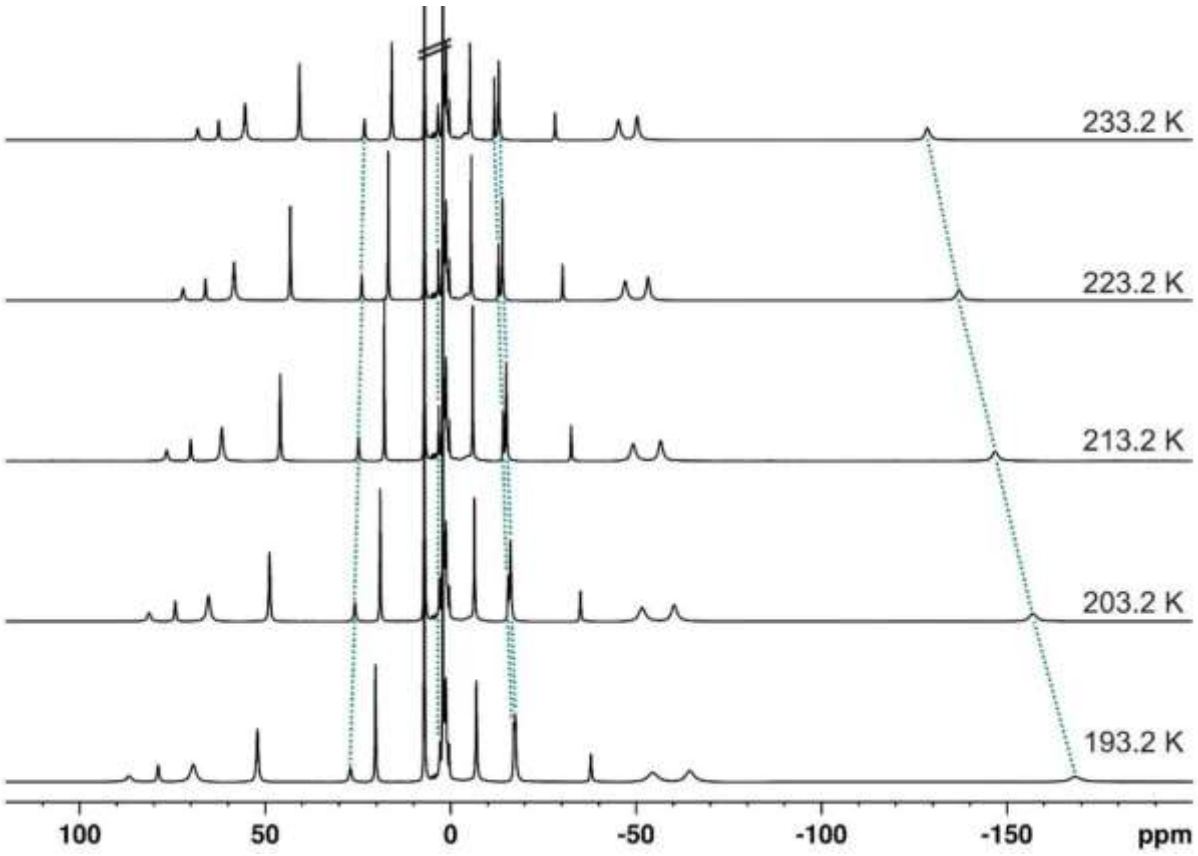

Figure S2. Variable-temperature ^{1}H NMR spectra of complex **1** (toluene-*d8*, 193.2 K to 233.2 K). Guidelines for the eyes provided for selected signals.

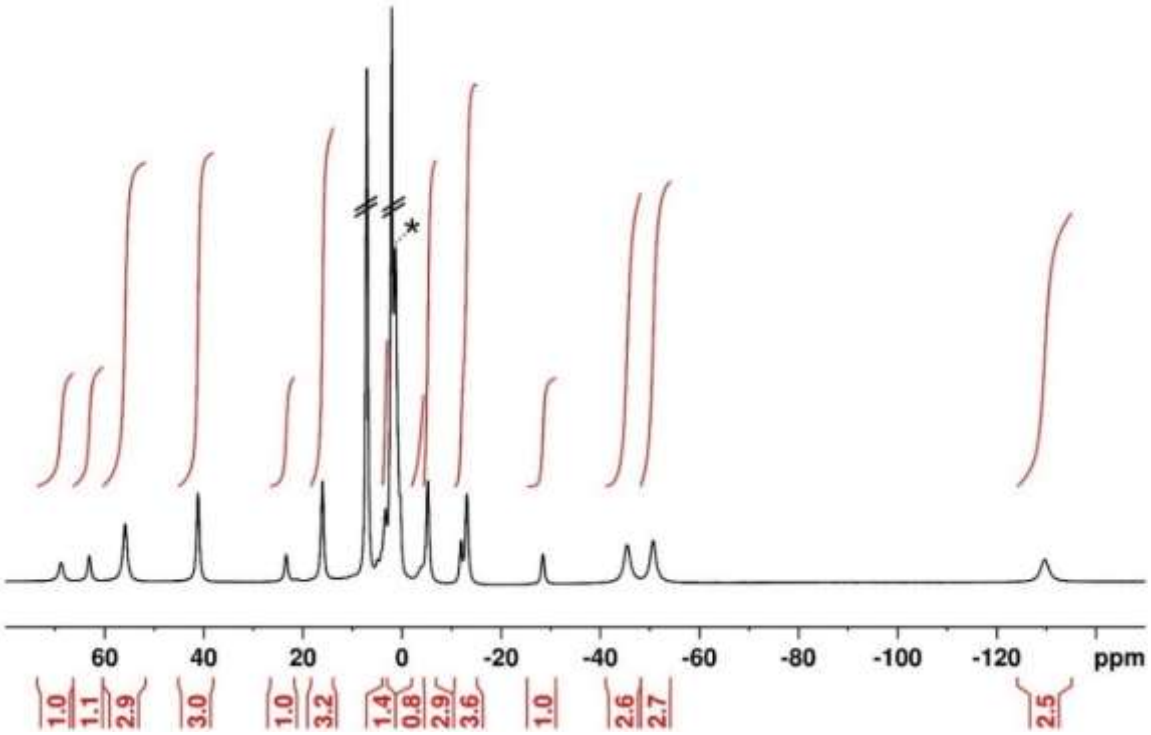

Figure S3. ^{1}H NMR spectrum of compound **1** (toluene-*d8*, 233.2 K). The integrals and their values are shown for the observed paramagnetic signals. The excitation pulse was at 0 ppm. * Diamagnetic impurity.

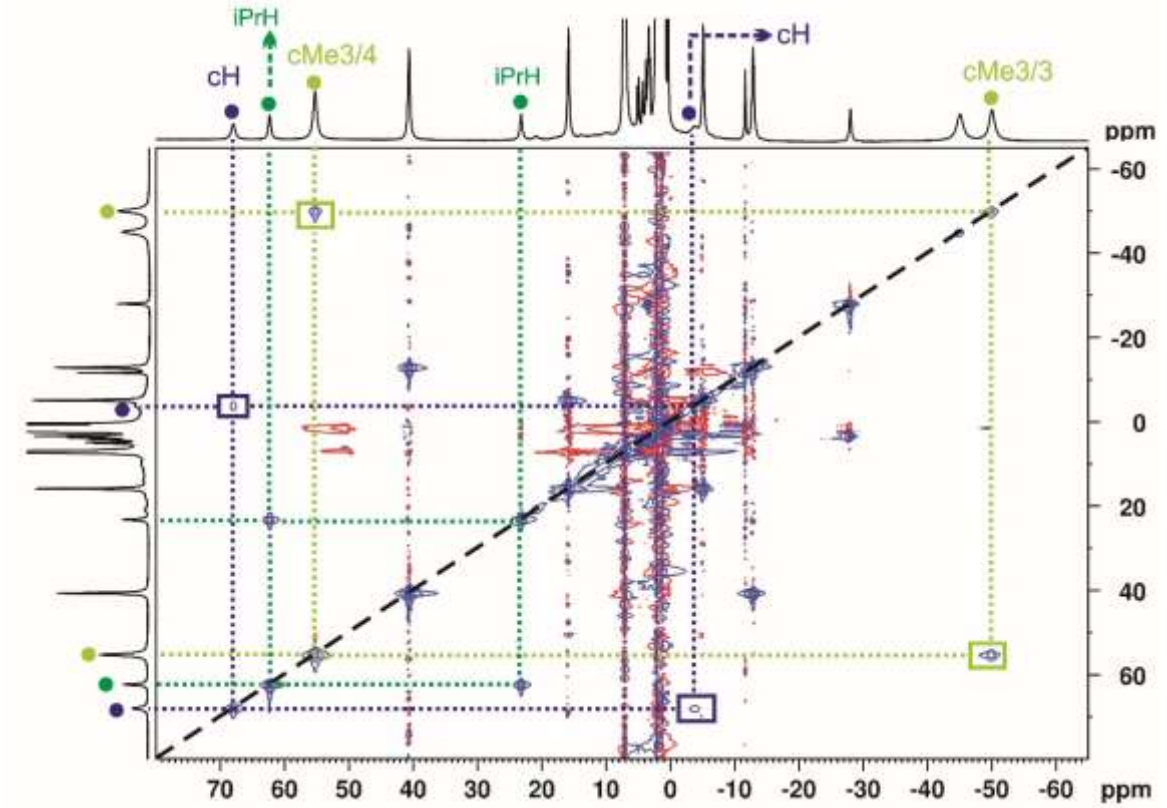

Figure S4. EXSY crosspeaks observed for two methyl groups and for two protons within a methylene group in cAAC of **1** (toluene-*d8*, 233.2 K, 9.4 T). Mixing time 5 ms.

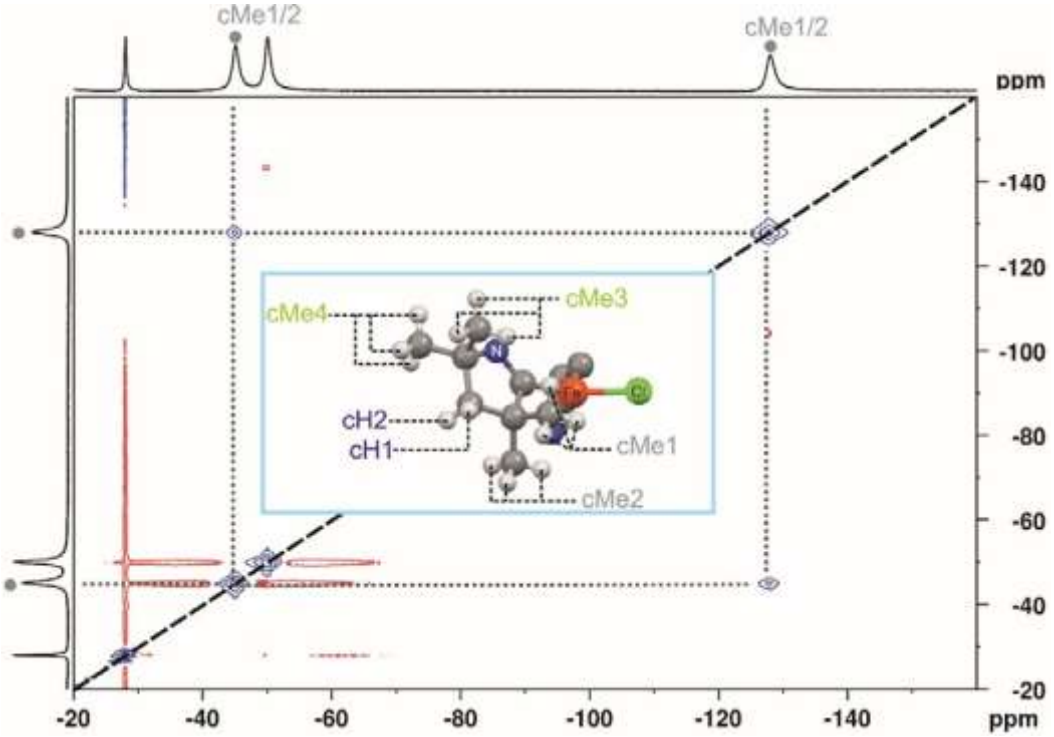

Figure S5. EXSY crosspeaks observed for two methyl group signals from cAAC in **1** (toluene-*d8*, 233.2 K, 9.4 T). Mixing time 1 ms.

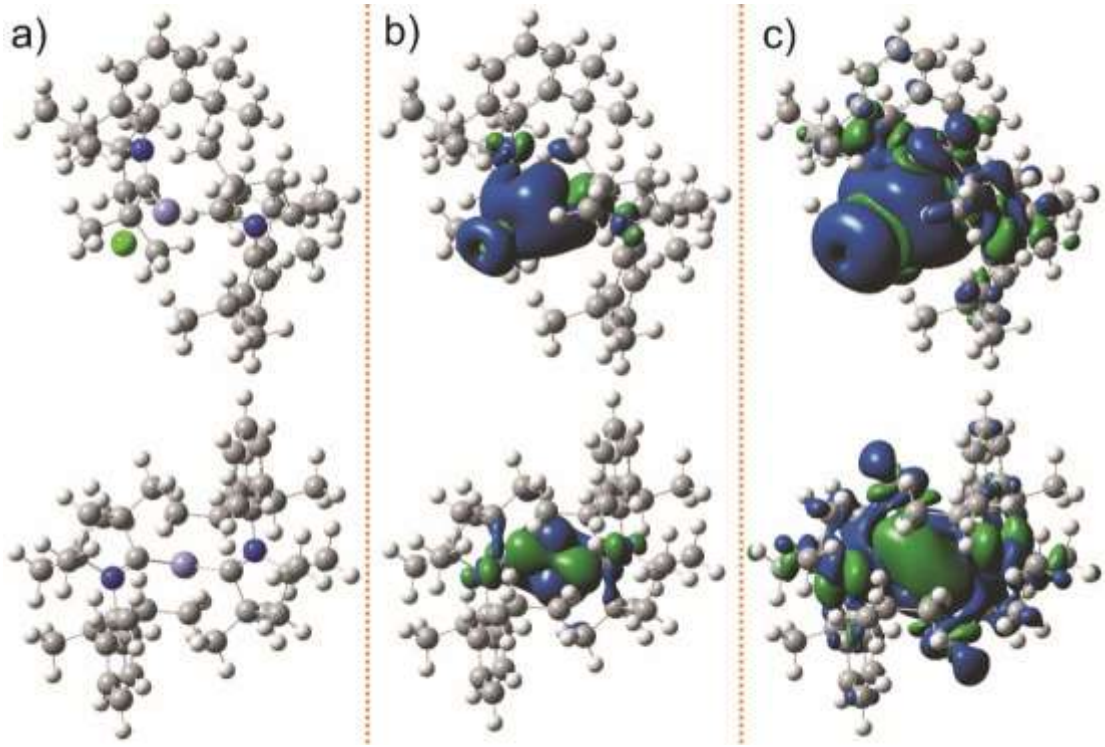

Figure S6. a) DFT optimized structure of **1** ($\mathcal{S} = 3/2$, ground state[1]). b) Spin-density distribution (isovalue 0.001). Considerable spin density can be seen on the N atoms and carbonyl C atoms. c) Spin-density distribution (isovalue 0.0001). Spin density of alternating sign can be seen in the aromatic part of the Dipp-moiety of the cAAC ligand, as well as on the iPr group. Positive spin density is given in blue, negative spin density is given in green color.

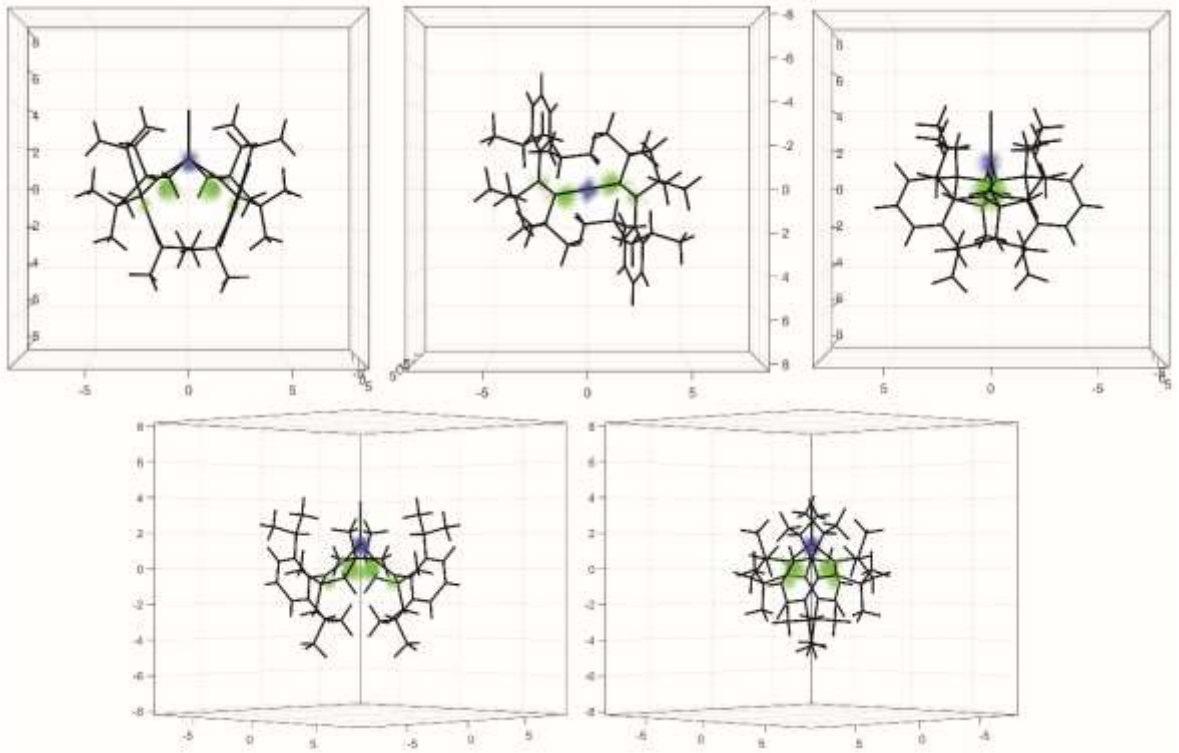

Figure S7. DFT-calculated spin density distribution in **1**. Positive spin density is given in blue, negative spin density is given in green color. The dimensions are given in Å. Created with Spinach.[2]

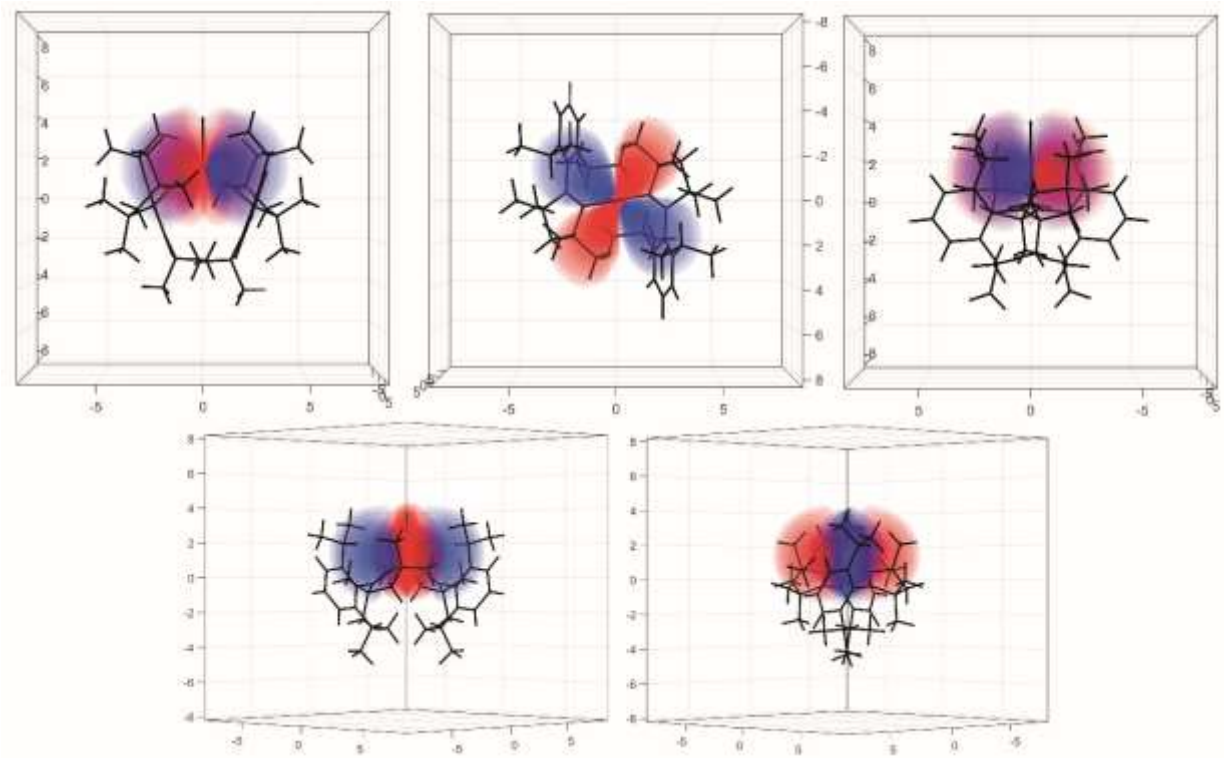

Figure S8. From the spin density (Figure S7) and the χ tensor calculated from DFT[3] (see above), this pseudocontact shift field of **1** was obtained. The dimensions are given in Å. Red: negative *PCS*, blue: positive *PCS*. Created with Spinach.[2]

As shown in Figure S8, DFT predicts a so-called rhombic pseudocontact shift field. The limiting case is when $\Delta\Delta\Delta_{rrh} = (2/3)\Delta\Delta\Delta_{aaaa}$ (ca. 67% of $\Delta\Delta\Delta_{aaaa}$). From the DFT calculated χ tensor, $\Delta\Delta\Delta_{aaaa}$ equals $1.57 \cdot 10^{-32}$ m^3, and $\Delta\Delta\Delta_{rrh}$ equals $-8.3 \cdot 10^{-33}$ m^3 (53% of $\Delta\Delta\Delta_{aaaa}$). With this tensor, the following pseudocontact shifts are predicted for the protons in the Dipp-moiety of the cAAC ligand of **1** (Figure 3, main text): iPrH1: +52.9 ppm, iPrH2: +1.05 ppm, oH1: +10.7 ppm, oH2:
+1.85 ppm, pH: +3.35 ppm. As will be shown in the analysis of experimental ^{1}H NMR shifts of **1**, the calculated χ tensor is not correct. However, it shows qualitatively that the iPrH protons have larger dipolar shifts than the oH and pH protons. In addition, the calculated *PCS* field shows why the ^{1}H NMR spectrum of **1** cannot be qualitatively interpreted as for cases when only the axial component of the magnetic susceptibility anisotropy is relevant.[4]

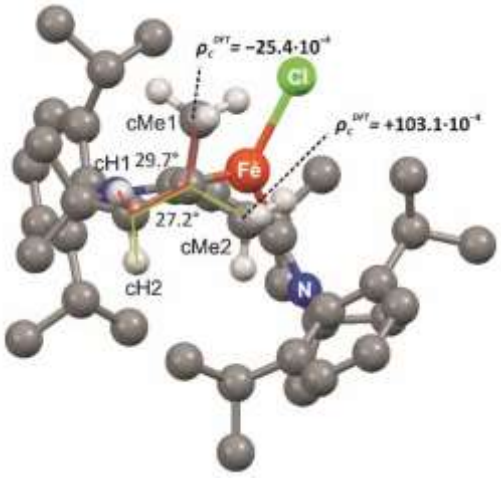

Figure S9. Relevant dihedral angles and ^{13}C spin densities ($\rho\rho_{CC}^{DDDDDD}$) in **1** which are expected to cause a discrepancy between the experimental and observed hyperfine terms for the resonances cH1 and cH2. Non-relevant hydrogen atoms omitted for clarity.

Details about the fitting of the ΔΔ tensor to the experimental pseudocontact shifts.

First, the assignment of the signals was established by using the DFT optimized structure of **1** and the experimental pseudocontact shifts of the resonances pH, mH1, mH2, iPrH1 and iPrH2. Permutations of the assignments of the pairs of signals (mH1 and mH2, iPrH1 and iPrH2) were done and the point-dipole based equation was used for locating the position of the Fe(I) ion for each permutation. The agreement between the calculated and experimental pseudocontact shift values (for fitted and remaining signals) and the located position of the Fe(I) ion (compared to the coordinates from the DFT optimized structure) were used to establish the correct signal assignment which is given in the main body of the paper. Differences between calculated and experimental pseudocontact shift values of approximately ±3 ppm and differences in the position of the Fe(I) ion in either (x, y or z) direction of maximum ±0.1 Å were tolerated. The positioning of the Fe(I) ion proved to be very valuable in finding the correct signal assignment, as the established to be wrong signal assignments showed deviations in the expected position of the Fe(I) ion by approximately ± 1 Å in most cases. A further refinement of the $\Delta\Delta$ was done by introducing the coordinates of the cH1 and cH2, as described in the main text.

Secondly, when the assignment of the ^{1}H resonances was established as described above, the distributed model which accounts for the delocalization of the unpaired electrons was used to calculate the pseudocontact shift contributions with the fitted $\Delta\Delta$ tensor.[3b]

Details about the axis frame of the D and ΔΔ tensors.

The following formalism was utilized for the ZFS parameters reported in this work: $-1/3 \leq E/D \leq +1/3$; $D = D_z - 0.5*D_x - 0.5*D_y$; $E = 0.5*(D_x - D_y)$; D_z, D_x and D_y are components of a traceless, diagonal tensor.[5] The individual components (obtained from experimental pseudocontact shift values) are D_x : -26.7 cm^{-1}: , D_y : -10.5 cm^{-1}, Dz : $+37.2$ cm^{-1}.

The following formalism was utilized for the $\Delta\Delta$ tensor (also a traceless diagonal tensor): axial component equals $\Delta\Delta_{zzzz} - (0.5*\Delta\Delta_{aaaa}) - (0.5*\Delta\Delta_{yyyy})$; rhombic component equals $\Delta\Delta_{aaaa} - \Delta\Delta_{yyyy}$. The values obtained from the experimental pseudocontact shift data were found to be $\Delta\Delta_{zzzz}$: -0.0853 Å^3, $\Delta\Delta_{aaaa}$: $+ 0.0715$ Å^3, $\Delta\Delta_{yyyy}$: $+ 0.0138$ Å^3.

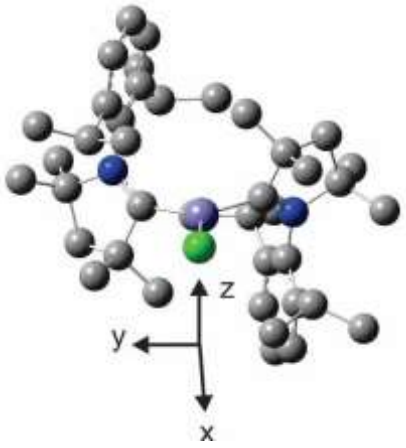

Figure S10. Directions of the principal axes of the $\Delta\Delta$ and D tensors utilized in this work. The xy plane contains the Fe(I) ion, the two carbon atoms and the chlorido ligands bonded to it, and the x axis points along the Fe(I)-Cl bond.

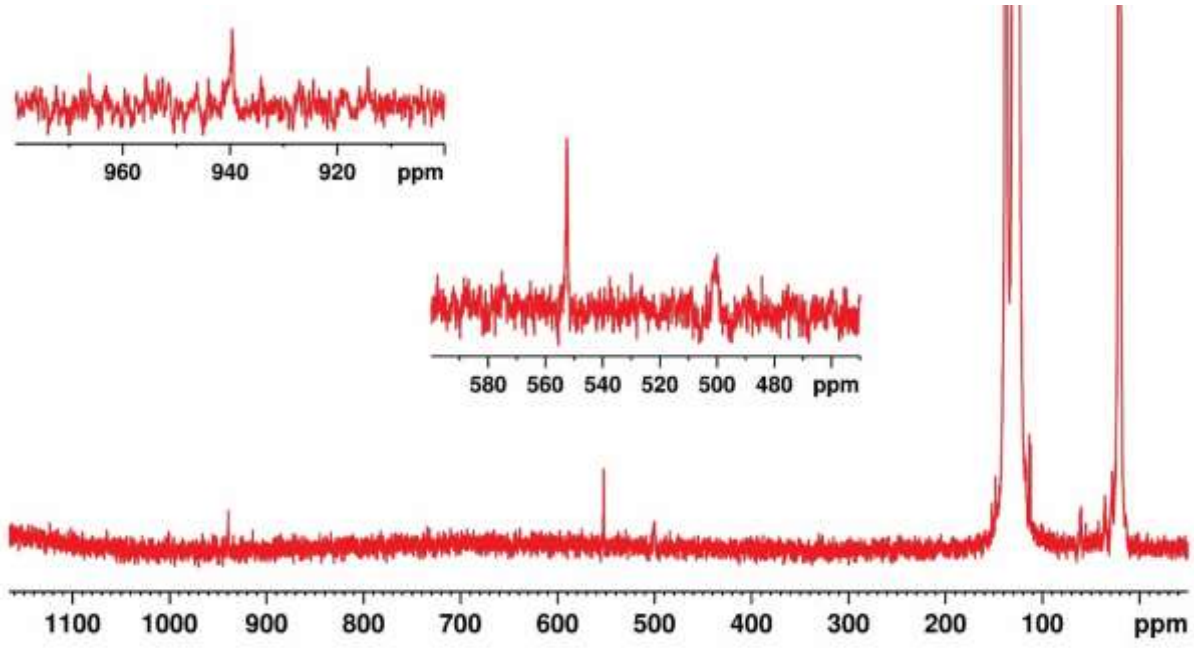

Figure S11. ^{13}C NMR spectrum of complex **1** (toluene-*d8*, 238.0 K, 14.09 T). Excitation pulse at +500 ppm. Insets show enlarged regions in which paramagnetic signals were observed.

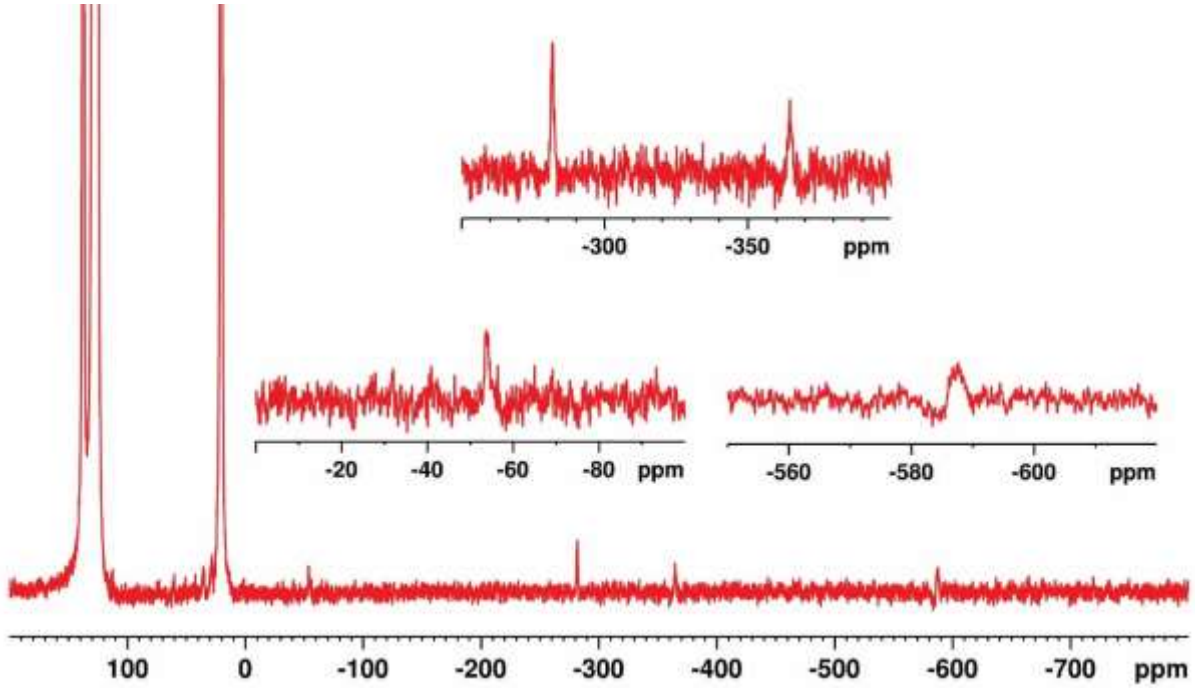

Figure S12. ^{13}C NMR spectrum of complex **1** (toluene-*d8*, 238.0 K, 14.09 T). Excitation pulse at -500 ppm. Insets show enlarged regions in which paramagnetic signals were observed.

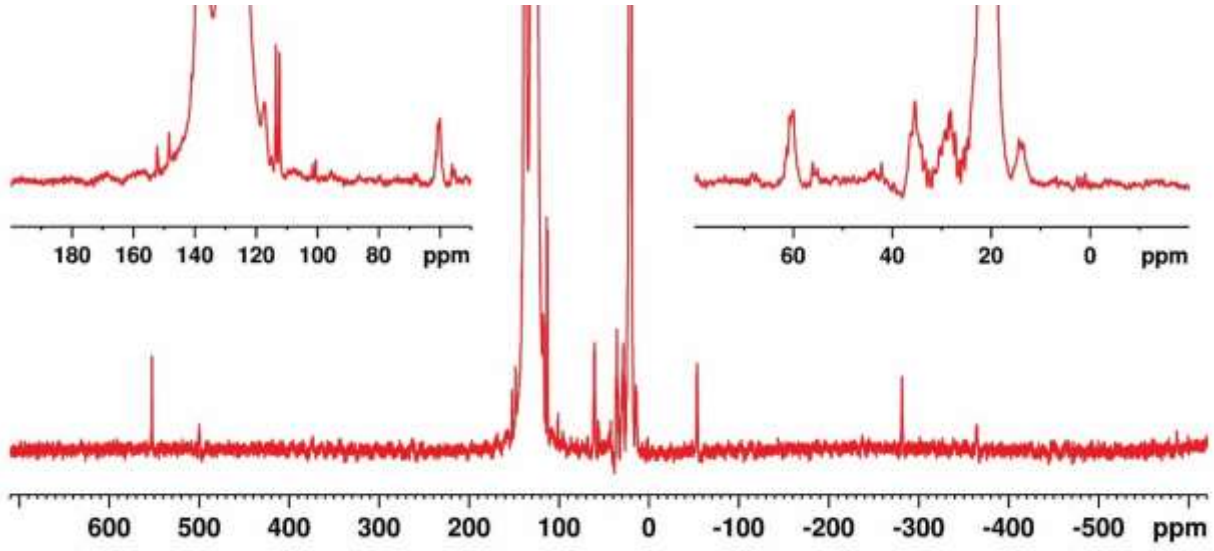

Figure S13. ^{13}C NMR spectrum of complex **1** (toluene-*d8*, 238.0 K, 14.09 T). Excitation pulse at +100 ppm. Insets show enlarged regions in which signals were observed.

The 14 observed ^{13}C NMR signals from the spectra above (besides toluene-*d8*) are listed here: +939.6 ppm, +552.3 ppm, +499.6 ppm, +152.1 ppm, +148.4 ppm, +113.0 ppm, +60.5 ppm, +35.5 ppm, +28.6 ppm, +14.0 ppm, -53.8 ppm, -281.4 ppm, -364.5 ppm, -588.6 ppm. A total of 20 signals were expected in the ^{13}C NMR spectrum of **1** (Figure S14). It is possible that some paramagnetic signals are under the very intense signals of the solvent molecules.

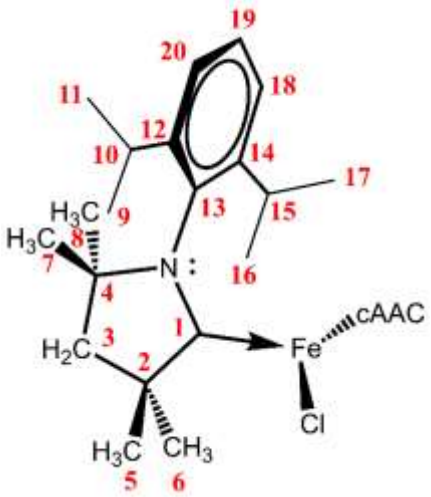

Figure S14. Different ^{13}C NMR resonances in complex **1**.

The calculated ^{13}C NMR chemical shifts of **1** are tabulated here. The chemical shift values were obtained as the sum of the diamagnetic terms (from reference compound, see main text), the Fermi-contact terms obtained with DFT calculated spin densities and the pseudocontact terms calculated with the fitted χ tensor and the equation from Kuprov *et al.* (whilst neglecting the small change in temperature between the studied ^{1}H NMR and ^{13}C NMR spectrum, i.e. 233.2

K vs. 238.0 K).[3b] Upon comparison with the observed signals in the ^{13}C NMR, a satisfactory agreement between theoretically calculated and experimentally observed chemical shifts is found. This is shown in Figure S15.

^{13}C Atom:	δ_{calc} [ppm]
1	121.6
2	2461.4
3	470.2
4	1154.4
5	-597.9
6	2578.6
7	-513.8
8	116.5
9	-212.2
10	212.9
11	59.7
12	-138.0
13	623.9
14	69.6
15	39.9
16	-276.5
17	37.4
18	72.8
19	152.4
20	80.2

Red color denotes calculated chemical shifts for which no resembling experimental chemical shift was observed. Green color denotes calculated chemical shifts for which resembling signals were observed in the NMR spectrum. The experimentally not observed signals are expected to be either too broad due to the proximity to the Fe(I) ion (^{13}C atoms 1, 5 and 6), experiencing very large Fermi-contact shifts (2, 6) covered by the intense signals of the solvent (18, 20).

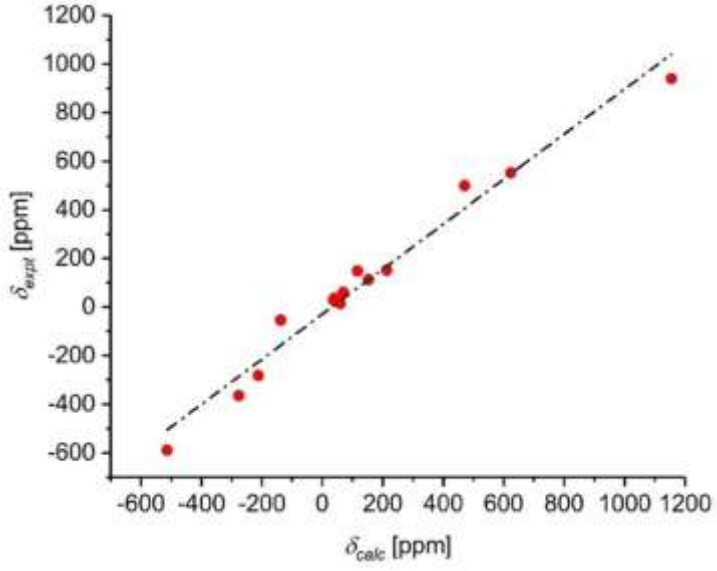

Figure S15. Plot of calculated ^{13}C NMR chemical shifts vs. chemical shifts of experimentally observed signals. Slope: 0.9264, intercept: -29.21 ppm, r^2: 0.9728. If the intercept is set to zero, slope: 0.9051, r^2: 0.9673.

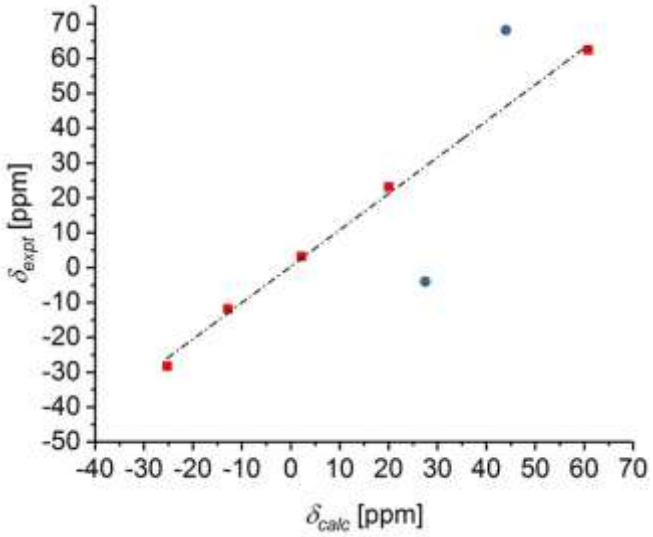

Figure S16. Plot of calculated ^{1}H NMR chemical shifts vs. chemical shifts of experimentally observed signals. Red points: resonances pH, mH1, mH2, iPrH1 and iPrH2. Blue points: resonances cH1 and cH2. A straight line has been fitted through the red points. Slope: 1.044, intercept: 0.363 ppm, r^2: 0.9967.

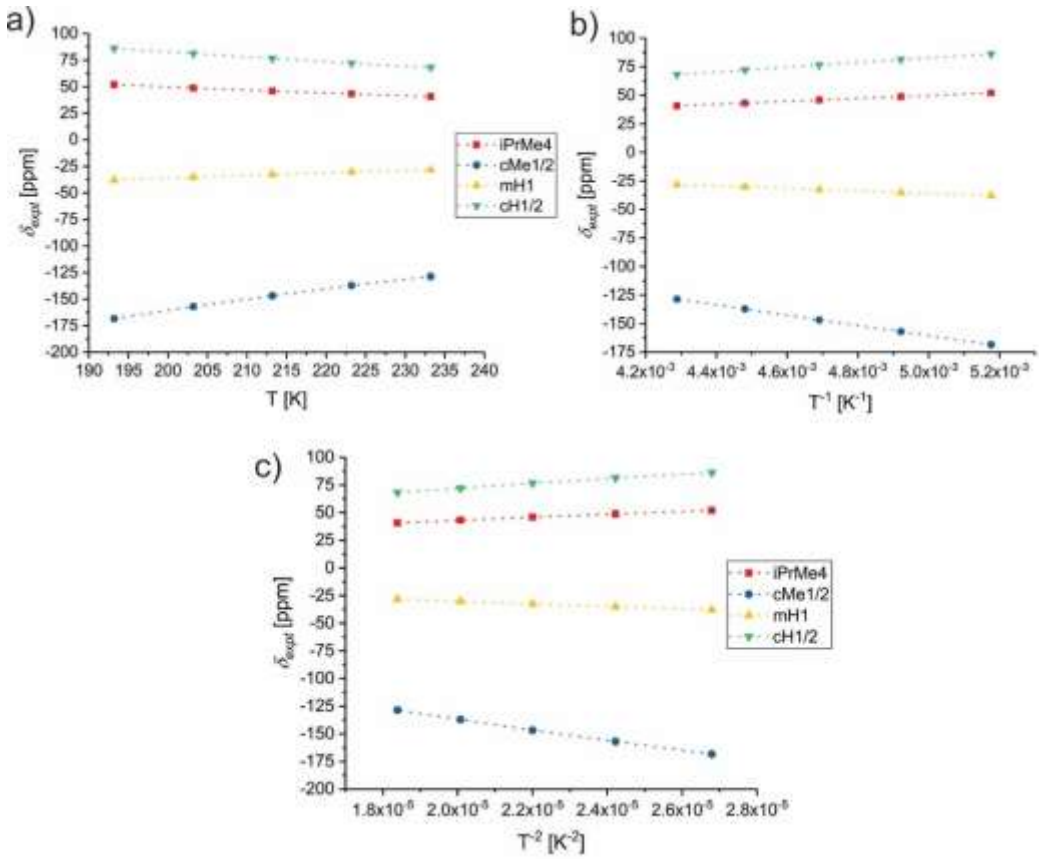

Figure S17. Plots of experimental chemical shift for selected ^{1}H resonances of complex **1** versus a) T; b) 1/T; c) $1/T^2$. Results of linear fittings to these plots are shown in the following Figures S18-S20.

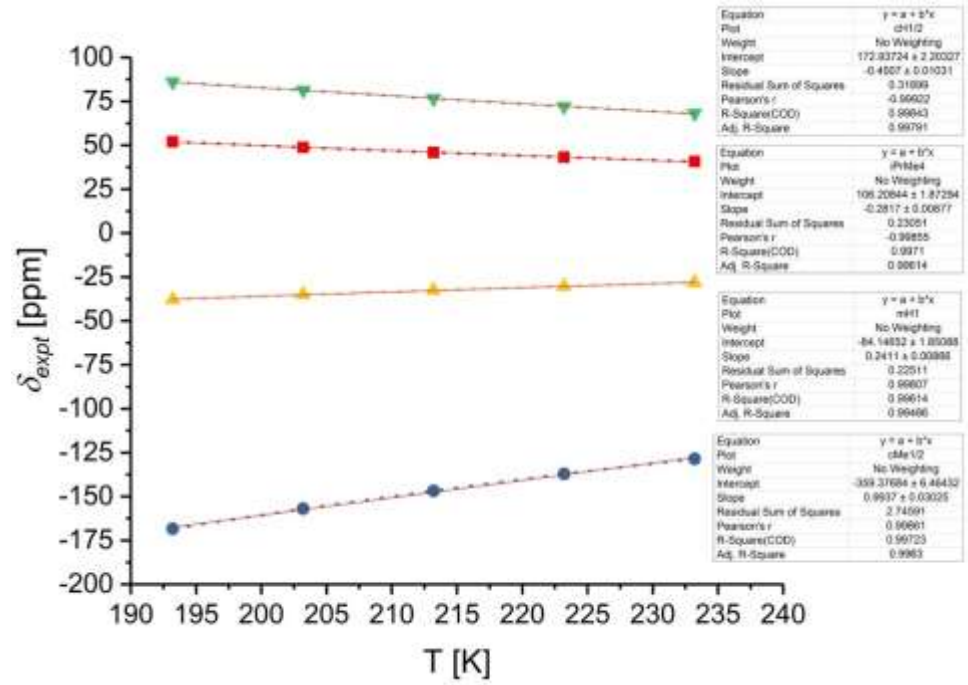

Figure S18. Linear fit of data from Figure S17 a).

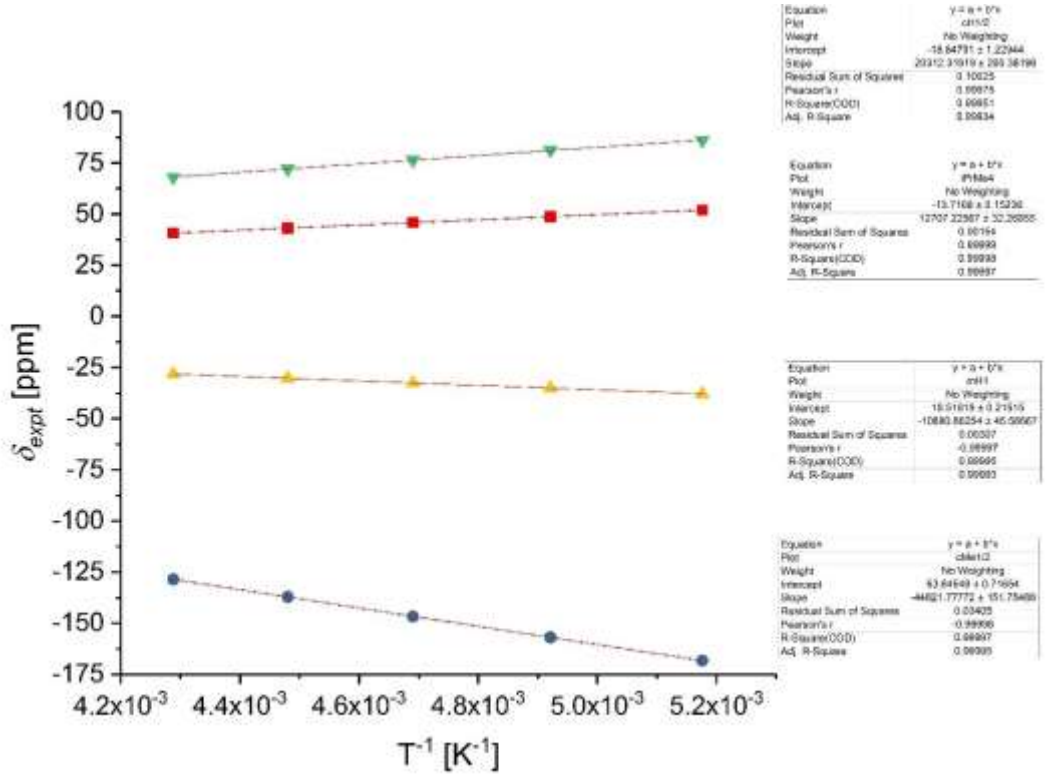

Figure S19. Linear fit of data from Figure S17 b).

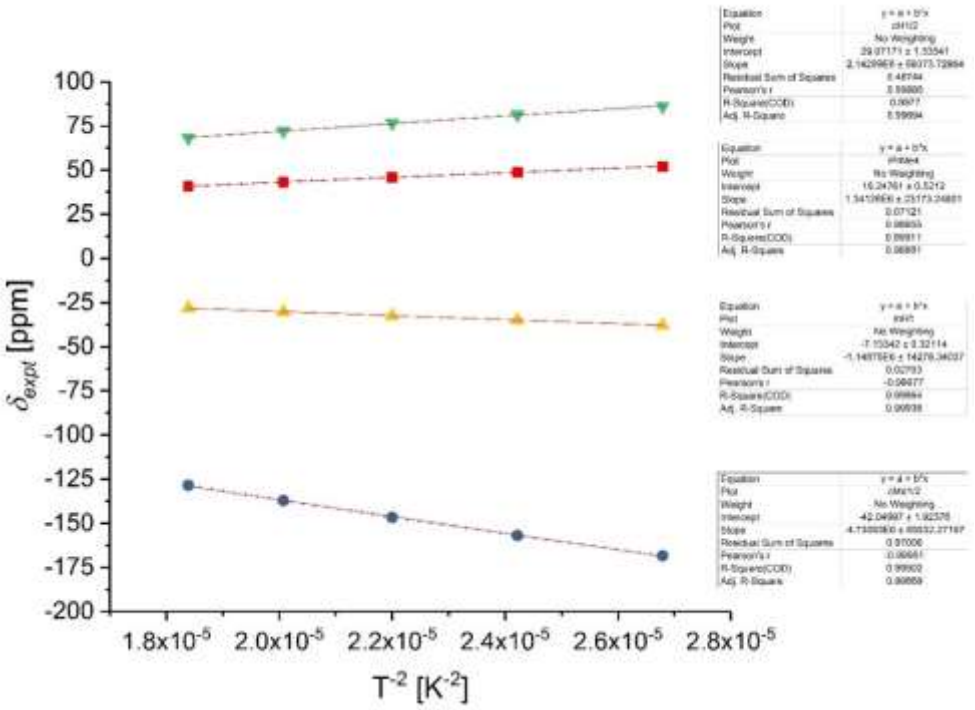

Figure S20. Linear fit of data from Figure S17 c).

The chemical shift data follows both 1/T and $1/T^2$ very well. However, results of linear fittings of the experimental chemical shift values show that these agree somewhat better with a 1/T dependence.

Spin density values obtained from DFT relevant for the calculation of Fermi-contact shifts. Values given for methyl groups have been averaged (see main text).

H Atom:	ρ [a. u.]
cH1	1.2E-4
cH2	1.0E-5
cMe1	-1.0E-5 2.4E-4 -2.0E-5
cMe2	-9.0E-5 8.7E-4 8.8E-4
cMe3	-3.0E-5 2.0E-5 -2.7E-4
cMe4	5.0E-5 3.1E-4 1.0E-5
oH1	0
oH2	0
pH	-1.0E-5
iPrH1	8.0E-5
iPrH2	1.0E-5
iPrMe1	-3.0E-5 7.0E-5 3.0E-5
iPrMe4	-4.0E-5 -1.0E-5 1.0E-5
iPrMe2	5.0E-5 1.0E-5 0
iPrMe3	0 0 1.0E-5

XYZ coordinates of DFT optimized structure of **1** used in this work:

106

Cl	0.000000	0.000000	3.781300
N	0.382600	2.475000	-0.349500
Fe	0.000000	0.000000	1.429800
N	-0.382600	-2.475000	-0.349500
C	-0.274400	1.619200	0.427000
C	-1.689000	2.130600	0.600900
C	-1.850900	3.197600	-0.496000
H	-2.303300	2.751700	-1.386100
H	-2.483100	4.032900	-0.186200
C	-0.424500	3.669500	-0.830400
C	-2.692400	0.978800	0.534100
H	-3.701800	1.327800	0.771500
H	-2.433700	0.214200	1.276800
H	-2.712000	0.494500	-0.439500
C	-1.782600	2.735500	2.017500
H	-2.792900	3.125100	2.179100
H	-1.076900	3.553300	2.165700
H	-1.567100	1.971400	2.766500
C	0.000000	4.929700	-0.070900
H	-0.611000	5.773500	-0.400100
H	1.044200	5.164500	-0.288300
H	-0.115400	4.826500	1.006000
C	-0.253700	3.954500	-2.320800
H	-0.606700	3.132200	-2.942700
H	0.789400	4.166900	-2.562900
H	-0.841300	4.840800	-2.572800
C	1.814300	2.406900	-0.496300
C	2.634100	2.790200	0.584300
C	4.019200	2.751000	0.408900
H	4.660400	3.049400	1.231000
C	4.589800	2.331100	-0.782600
H	5.668700	2.311800	-0.896000
C	3.769100	1.912800	-1.818600
H	4.211800	1.544900	-2.738000
C	2.379000	1.934400	-1.696200
C	2.105200	3.197900	1.946400
H	1.017000	3.139300	1.928200
C	2.525200	4.626600	2.328600
H	2.232400	5.361300	1.577400
H	3.609600	4.691700	2.453900
H	2.066200	4.907500	3.280600
C	2.593400	2.218800	3.023500
H	2.174100	2.487700	3.995600
H	3.684200	2.237100	3.103100
H	2.271800	1.200300	2.809800
C	1.553000	1.360400	-2.828900
H	0.507500	1.549400	-2.604100
C	1.885600	1.986300	-4.191000
H	1.177800	1.634700	-4.947300
H	2.887000	1.699800	-4.523500
H	1.842800	3.076200	-4.164400
C	1.731900	-0.163100	-2.904700
H	1.334600	-0.640600	-2.008700
H	2.788100	-0.429900	-3.000200
H	1.204900	-0.564100	-3.775000
C	0.274400	-1.619200	0.427000
C	1.689000	-2.130600	0.600900
C	1.850900	-3.197600	-0.496000
H	2.303300	-2.751700	-1.386100
H	2.483100	-4.032900	-0.186200
C	0.424500	-3.669500	-0.830400
C	2.692400	-0.978800	0.534100
H	2.712000	-0.494500	-0.439500
H	3.701800	-1.327800	0.771500
H	2.433700	-0.214200	1.276800
C	1.782600	-2.735500	2.017500
H	1.076900	-3.553300	2.165700
H	1.567100	-1.971400	2.766500
H	2.792900	-3.125100	2.179100
C	0.253700	-3.954500	-2.320800
H	-0.789400	-4.166900	-2.562900
H	0.841300	-4.840800	-2.572800
H	0.606700	-3.132200	-2.942700
C	0.000000	-4.929700	-0.070900
H	-1.044200	-5.164500	-0.288300
H	0.115400	-4.826500	1.006000
H	0.611000	-5.773500	-0.400100
C	-1.814300	-2.406900	-0.496300
C	-2.634100	-2.790200	0.584300
C	-4.019200	-2.751000	0.408900
H	-4.660400	-3.049400	1.231000
C	-4.589800	-2.331100	-0.782600
H	-5.668700	-2.311800	-0.896000
C	-3.769100	-1.912800	-1.818600
H	-4.211800	-1.544900	-2.738000
C	-2.379000	-1.934400	-1.696200
C	-2.105200	-3.197900	1.946400
H	-1.017000	-3.139300	1.928200
C	-2.593400	-2.218800	3.023500
H	-3.684200	-2.237100	3.103100
H	-2.271800	-1.200300	2.809800
H	-2.174100	-2.487700	3.995600
C	-2.525200	-4.626600	2.328600
H	-3.609600	-4.691700	2.453900
H	-2.066200	-4.907500	3.280600
H	-2.232400	-5.361300	1.577400
C	-1.553000	-1.360400	-2.828900
H	-0.507500	-1.549400	-2.604100
C	-1.885600	-1.986300	-4.191000
H	-1.842800	-3.076200	-4.164400
H	-1.177800	-1.634700	-4.947300
H	-2.887000	-1.699800	-4.523500
C	-1.731900	0.163100	-2.904700
H	-2.788100	0.429900	-3.000200
H	-1.204900	0.564100	-3.775000
H	-1.334600	0.640600	-2.008700

References for ESI

1. P. P. Samuel, K. C. Mondal, N. Amin Sk, H. W. Roesky, E. Carl, R. Neufeld, D. Stalke, S. Demeshko, F. Meyer, L. Ungur, L. F. Chibotaru, J. Christian, V. Ramachandran, J. van Tol and N. S. Dalal, *J. Am. Chem. Soc.*, 2014, **136**, 11964-11971.
2. H. J. Hogben, M. Krzystyniak, G. T. Charnock, P. J. Hore and I. Kuprov, *J. Magn. Reson.*, 2011, **208**, 179-194.
3. a) T. A. Keith and R. F. W. Bader, *Chem. Phys. Lett.*, 1993, **210**, 223-231; b) G. T. Charnock and I. Kuprov, *Phys. Chem. Chem. Phys.*, 2014, **16**, 20184-20189.
4. M. Damjanovic, K. Katoh, M. Yamashita and M. Enders, *J. Am. Chem. Soc.*, 2013, **135**, 14349-14358.
5. D. Gatteschi, R. Sessoli and J. Villain, *Molecular Nanomagnets*, Oxford University Press, New York, 2006.